www.serd.ait.ac.th/reric

Development of a Wind Turbine Simulator for Wind Generator Testing

Bunlung Neammanee*1, Somporn Sirisumrannukul* and Somchai Chatratana+

Abstract - *The paper presents the development of a wind turbine simulator which consists of an induction motor driven by a torque control inverter. The wind turbine simulation system includes wind speed simulation, mathematical models of wind turbines, modeling of rotor blade characteristics, modeling of tower effect and emulation of rotor inertia. Wind speed can be easily programmed based on Van der Hoven spectrum, or recorded wind speed data or manual set up. The developed algorithms were implemented by a low-cost, high-performance digital signal controller with C language and the system was tested in a laboratory with a 1 kW dc generator. The power responses, torque responses and tip speed ratio responses confirms that the system can perform satisfactorily under step changes of power reference, load disturbances and tower effect.*

Keywords **- Wind turbine simulator, Wind speed generation, Power spectrum, Torque control.**

1. INTRODUCTION

Wind power has become one of the most attractive energy resources for electricity production as it is virtually pollution-free (if noise is not considered as pollution). As a result, a great deal of research has been focused on the development of new turbine design to reduce the costs of wind power and to make wind turbines more economical and efficient. The investigation of wind power system involves high performance wind turbine simulators, especially for the development of optimal control solutions. At present, wind turbine simulators have become a necessary tool for research laboratories to enhance the quality of the wind energy conversion system.

The basic requirement for a wind simulator is that its static and dynamic characteristics must be as close as possible to those of a real wind turbine. For the last few decades, the most common structure of wind simulators was based on the DC motor with current control (i.e., torque control on its shaft) as a prime mover. However, the simulator requires a relatively large-sized DC motor. This constraint makes DC motor system unattractive, due to its unavailability and maintenance requirement. In addition, it is rather expensive. Later the DC motor system was replaced by an induction motor system which eliminated the above mentioned disadvantages.

In this paper, a squirrel cage induction motor is proposed for a wind simulator as a torque-generating source. The wind simulator consists of two main parts as shown in Fig 1. The first part (left hand side of the figure) is used to create required wind speed. The power-speed pattern of the wind can be generated from the data based on the Van der Hoven power spectrum or from the actual recorded wind speed data or from manual set up. This part includes the mathematical model of the wind turbine to calculate reference signals which will be used as torque reference for an torque control inverter in the second part. The second part is an electromechanical tracking system which generates the shaft torque whose characteristics are governed by the pattern determined by the first part.

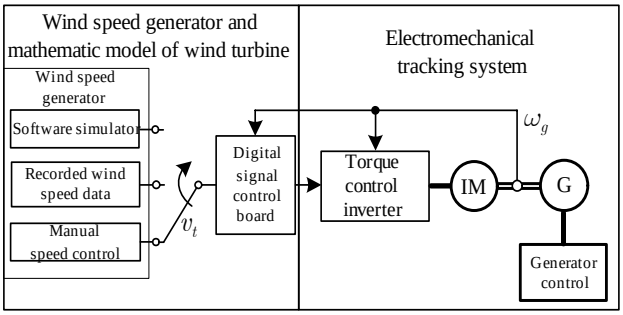

Fig. 1. Purposed wind speed simulator.

The developed wind turbine simulator employs a 4-kW induction motor as prime mover. A digital signal controller (DSC) board is used to interface the wind speed generator and the inverter which drives the induction motor. The DSC board is connected with a personal computer for data acquisition to verify control algorithms and display relevant parameters.

2. WIND SPEED SIMULATION

Wind speed simulation is important in determining the performances of wind generators and the features offered by a simulator for predicting the energy output and analysis of the energy conversion and system dynamics. The nature of wind speed is generally composed of two components: steady state mean flow and turbulence. These two

*Department of Electrical Engineering, Faculty of Engineering, King Mongkut's Institute of Technology North Bangkok, Thailand, Pibulsongkram Rd., Bangsue, Bangkok 10800, Thailand.

+Technology Management Center, National Science and Technology Development Agency (NSTDA), 111 Thailand Science Park, Paholyothin Rd., Klong 1, Klong Luang, Phathumthani 12120, Thailand.

1Corresponding Author:
E-mail: bln@kmitnb.ac.th

components are normally simulated separately. The mean component is the steady part of temporal average over period and increases with elevation. The turbulence component is characterized by random fluctuation with the mean component and with time and space. The turbulence component is commonly considered a stationary Gaussian process.

As wind speed data are time series, identificating the data can be captured in forms of time and frequency domains. In this paper, the frequency power spectrum based on the Van der Hoven spectrum shown in Fig. 2 is adopted [1], [2]. This spectrum is regarded as one of the best known reference of wind speed spectrum. In the frequency domain, the equivalent description of wind fluctuation component can be obtained through power spectrum density and coherence functions. The figure is divided into low frequency component and high frequency component. The former generates the mean wind speed whereas the latter generates the turbulence.

The Van der Hoven spectrum in Fig. 2 shows the contribution of harmonic components in a range from 0.0007 to 900 cycles/h (i.e., more than six decades). This spectrum gives a complete description of the energy content of turbulence. The frequency range contains the spectrum domain that describes the medium and long-term variations, as well as the spectrum range of the turbulent component. From the Van der Hoven spectrum, a numerical wind speed simulation procedure has been developed based on the sampling of the spectrum. For every value of discrete angular frequency ω_i, $i = 1,2,...N+1$ the spectrum gives a corresponding value of power spectrum density, $S_{vv}(\omega_i)$. The amplitude A_i at frequency ω_i is given by

$$A_i = \sqrt{\frac{1}{2}[S_{vv}(\omega_i) + S_{vv}(\omega_{i+1})](\omega_{i+1} - \omega_i)} \quad (1)$$

The wind speed, v_t, as a function of time is simulated by

$$v_t = A_0 + \sum_{i=1}^{N} A_i \cos(\omega t + \varphi_i) \quad (2)$$

with $A_0 = \overline{v}$, $\omega_0 = 0$ and $\varphi_0 = 0$. Note that the first and second terms of Equation (2) represent the average and turbulence of wind speed, respectively. The parameter $\overline{v}$ is calculated on a time horizon greater than the largest period in the Van der Hoven characteristic.

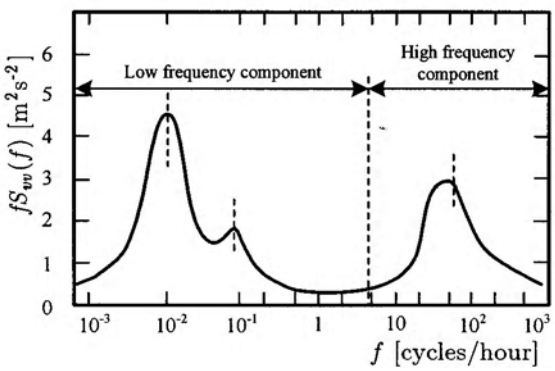

Fig. 2. Van der Hoven spectrum.

3. MATHEMATICAL MODEL OF WIND TURBINES

A horizontal wind turbine is coupled with a gear box to capture and transfer energy to the generator, is shown in Fig. 3 (a). Many wind turbines are directly coupled with low speed generator without a gear to reduce the gear's losses, weight and maintenances. A vertical wind turbine, shown in Fig 3 (b), has the same characteristics but it can be operated at a low tip speed ratio. The characteristics such as power, torque and speed for a wind turbine can be modeled by a motor and generator set with a motor torque controller. The controller uses a torque reference which is a function of wind speed, rotational speed and the aerodynamics of the rotor blades to generate a desired torque.

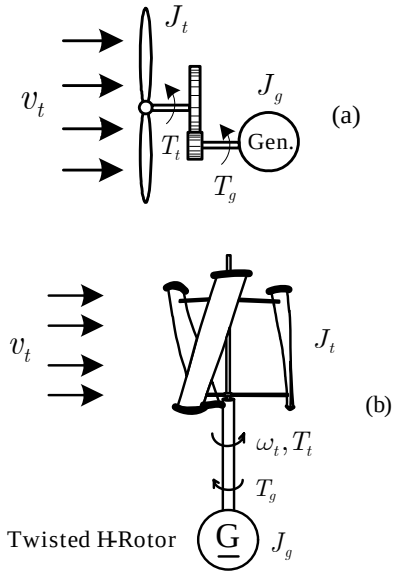

Fig. 3. a) Horizontal wind turbine coupling with gear box b) Vertical twisted-H Rotor with direct coupling to generator.

Modeling of Rotor Blade Characteristics

In general, wind speed varies more significantly with elevation of the blades than any other direction. Every single spot on the blades would not have the same wind speed owning to wind field impact. Therefore, it would be difficult if modeling of wind speed takes into account all different positions on the blades. For this reason, a single value of wind speed is normally applied to the whole wind turbines.

The power from an ideal wind turbine is calculated by a linear momentum theory [3] with the following assumptions: i) homogenous, incompressible, steady state fluid flow, ii) no friction drag, iii) an infinite number of blades, uniform thrust over the disk rotor blades and iv) a non rotational wake The power generated from the wind can be expressed by (3).

$$P_{wind} = \frac{\rho}{2} A_{turb} v_t^3 \quad (3)$$

According to Betz's law, an ideal wind turbine would, in theory, extract the 16/27 of this power. However, in practice, due to non-laminar air flow and friction between blade

surfaces, the energy capture of the wind turbine is reduced by a factor known as the power coefficient, c_P, given in (4). The power coefficient, also called the Bezt factor, is defined by

$$\text{power coefficient ; } c_p = \frac{\text{rotor power}}{\text{power of wind}} \tag{4}$$

For a real wind turbine (usually) with three aerodynamically designed blades, the power coefficient depends on the tip speed ratio, λ, defined by

$$\lambda = \frac{\omega_t R}{v_t} \tag{5}$$

The value of c_P is also a function of the pitch angle, β. Changing will affect lift and drag forces acting on the blades, thus changing the output power. Hence, the power captured by the blades, , is

$$P_{turb} = \frac{\rho}{2}\pi R^2 v_t^3 c_P(\lambda,\beta) \tag{6}$$

The aerodynamic torque acting on the blades, T_{turb}, is obtained by

$$T_{turb} = \frac{\rho}{2}\pi R^3 v_t^2 c_T(\lambda,\beta) \tag{7}$$

If c_P is known, the aerodynamic torque can also be calculated from

$$T_{turb} = \frac{\rho}{2}\pi R^2 v_t^3 c_P(\lambda,\beta)/\omega_t \tag{8}$$

In this paper, a constant value of β is of interest; namely, the pitch angle is fixed and this is generally true for small and medium sized wind turbines. Therefore, c_T and c_P depend only on λ.

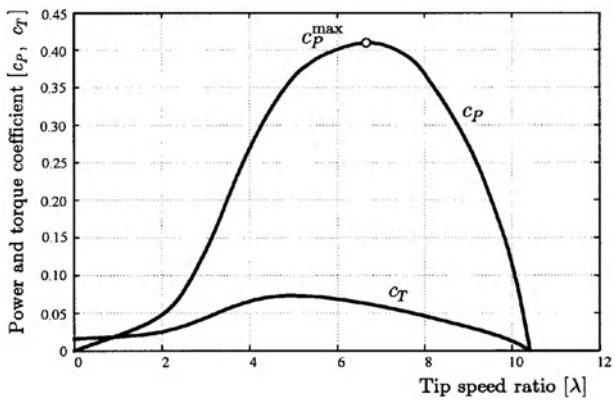

Fig. 4. $c_T - \lambda$ and $c_P - \lambda$ characteristics for a real 3 kW wind turbine.

Figure 4 shows the c_P curve as a function of λ of a real 3 kW, three blade horizontal axis wind turbine with a rotor diameter of 4.5 m [4], [5]. This curve represents an important characteristic which determines the starting torque of the wind turbine. In general, this curve is available from the manufacture or can be obtained from a field test. With the c_P curve, which indicates the efficiency of power conversion of the rotor blades, can be calculated by multiplying c_T with λ [6]. Figure 4 also shows the $c_T - \lambda$ profile corresponding to the curve. It is important to note that the power and torque coefficient of a wind turbine depends on aerodynamic design of the blades. With Equations (5), (7) and Fig. 4, a block diagram can be built as shown in Fig. 5.

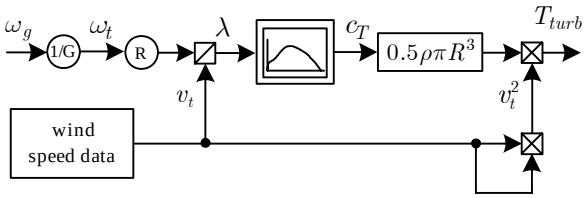

Fig. 5. Block diagram of rotor blade characteristics.

Periodic Torque Ripple Caused by Tower Effect

Theoretically, the rotor of a horizontal-axis wind turbine must rotate as closed as possible to the tower to limit the length of the nacelle [7] because an extremely protruding nacelle causes the rotor faces to act with great leverage to the tower axis. The upwind turbine is affected merely by a retardation of the flow in front of the tower, which is known as the bow-wave effect. If the clearance between the rotor blades and tower is small, the blow wave has more effect to the wind speed and makes more hazard if the rotor blades and tower have vibration. In practice, a minimum clearance of approximately one tower diameter ($x/D = 1$) is maintained for structural safety. With this clearance, the wind speed striking on the blade reduces approximately 10 %, as shown in Fig. 6.

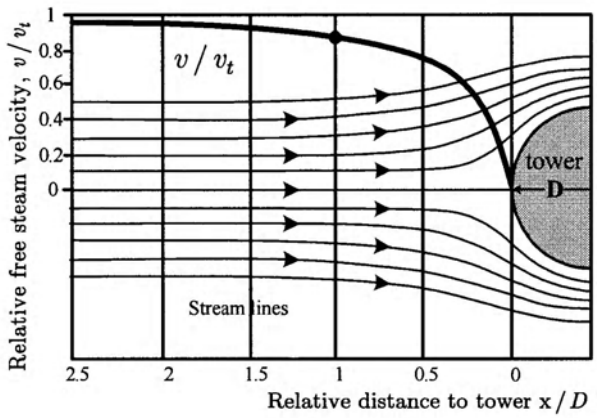

Fig. 6. Flow field ahead of a cylindrical tower for upwind.

The tower effect causes the output torque of a wind turbine to be periodically rippled torque [8]. The phenomenon can be graphically explained by Fig. 7a). As the wind passes through the tower, the wind speed in front of the tower decreases due to the resistance of the tower structure. At this time, if the tower and one of the blades are in alignment, the wind speed striking the blades will reduce and cause the ripple effect as shown in Fig. 7 b), where the shape of the torque ripple is modeled as a ramp function. The frequency of the torque ripple is equal to the rotational frequency multiplied by the number of blades. The shape and amount of the torque ripple depend on the physical structures of the blades and tower. The net output torque

taking the tower effect into account can be calculated by (9) and (10)

$$T_{turb} = T'_{turb} - T_{tower} \tag{9}$$

$$T_{turb} = (J_t + GJ_g)\alpha_t + GT_g + T_{f1} \tag{10}$$

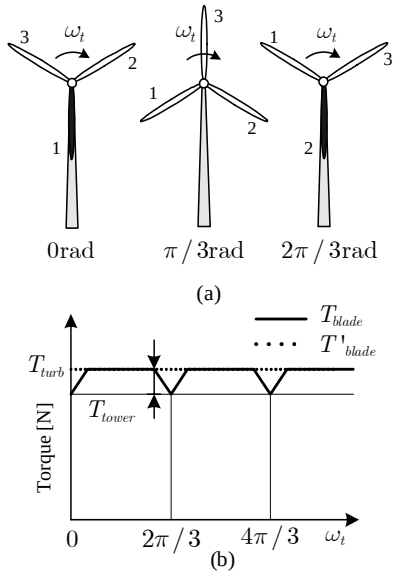

Fig. 7. (a) Rotor position at $\omega_t = 0,\ 2\pi/3,\ 4\pi/3$ rad (black blade creates the tower effect). (b) Ramp shape of torque ripple modeling for upwind tower effect.

Emulation of Rotor Inertia

Figure 8 shows the physical structure of a wind turbine consisting of blades (left part), a gear box (middle part), and a generator (right part). A torque equation of the wind turbine is given in Equation (10) with an assumption that all of the rotating parts are considered a lumped mass. Figure 9 shows the block diagram of the wind turbine, which is developed from Equations (5) and (10).

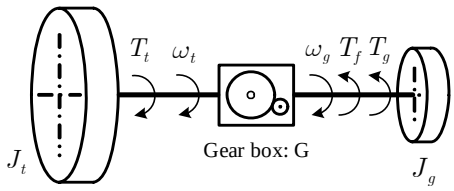

Fig. 8. System moment of inertia.

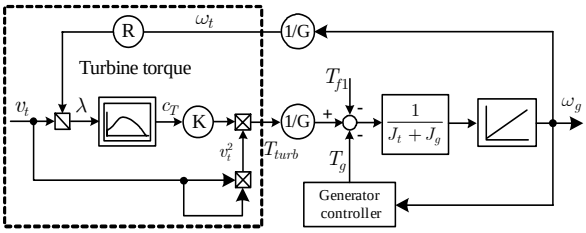

Fig. 9. Block diagram for the wind turbine and generator torques.

If an induction motor is employed in the wind turbine simulator, the torque behavior generated by motor should be similar to that generated by a real wind turbine. This can be achieved by a dynamic equation [9]

$$T_m = (J_m + GJ_g)\alpha_t + GT_g + T_{f2} \tag{11}$$

Subtracting (10) from (11) with the assumption that the friction and gear losses can be negligible (i.e., T_{f1} and T_{f2} =0) and rearranging gives

$$T_m = T_{turb} - (J_t - J_m)\alpha_t \tag{12}$$

$$T_{comp} = (J_t - J_m)\alpha_t \tag{13}$$

Figure 10 shows an extension of Fig. 9 to include the term ($J_t - J_m$) (compensation moment of inertia) and derivative of the rotational speed used to produce the compensation torque, T_{comp} . The compensation torque varies with the acceleration or deceleration of the wind turbine. A low pass filter (LPF) in the figure is included for noise elimination.

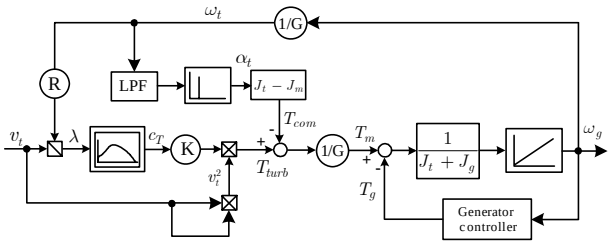

Fig. 10. Block diagram for compensation of the moment of inertia.

4. IMPLEMENTATION OF WIND SIMULATOR SYSTEM

Wind Simulator Hardware

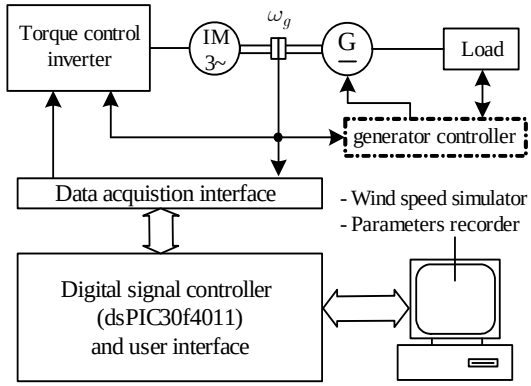

Fig. 11. Hardware structure of the wind turbine simulator.

The hardware components in Fig. 11 are composed of 1) three phase 4-kW induction motor coupled with 1 kW dc generator, 2) 1000 pulses rotary encoder, 3) torque control inverter, 4) Digital signal controller (DSC) board, and 5) a personal computer. The DSC board uses a high performance 16 bits dsPIC30f4011 which combines the advantage of high performance 16-bit microcontroller and high computation speed digital signal processors.

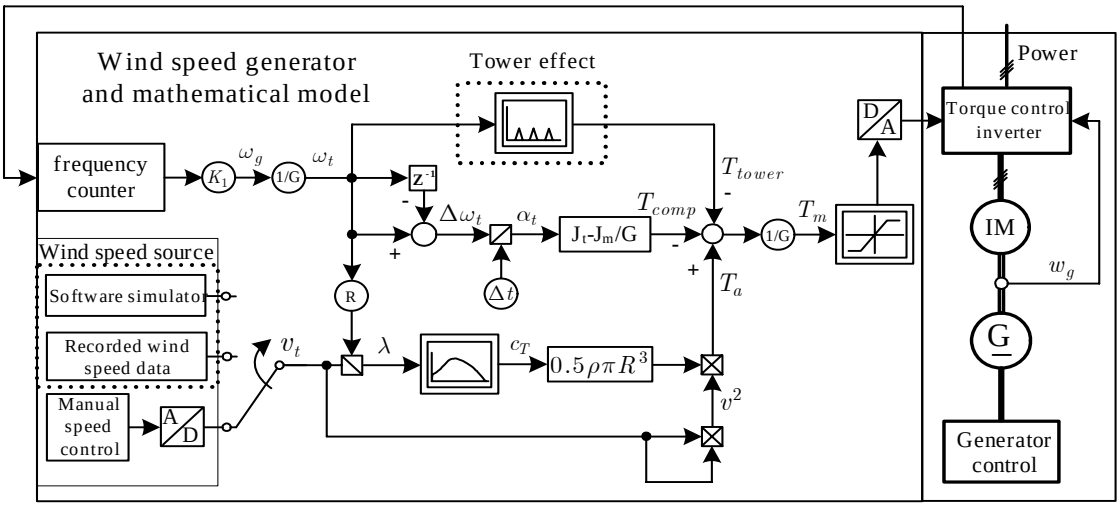

Fig. 12. Signal flow of wind simulator software.

Speed signal from the encoder is sent to the torque controller inverter and the DSC board via a data acquisition interface circuit inside the DSC board. The DSC board is linked with the personal computer via two RS232 ports: one port for transferring wind speed data to the DSC board and the other for sending the values of different parameters (P , ω_t , α_t , λ , c_T) to the computer.

Wind Simulator Software

Figure 12 shows a signal flow diagram of the software implemented on the DSC board. The command sets were programmed in C language. The algorithm starts by receiving rotational speed signal from the encoder and wind speed that can be selected from three sources as shown by a block at the lower end on the left hand corner of Fig. 12. The three sources are 1) manual input from a potentiometer, 2) a data file from a wind speed recorder and 3) the proposed software simulator, which is able to generate time-series wind speed such as the Van der Hoven. With wind speed data, the DSC is able to calculate parameters such as ω_g , λ and α_t . The parameter c_T , needed for the aerodynamic torque calculation, can be directly obtained from a look up table. The DSC computes the torque compensation and the periodic torque ripple due to the tower effect represented by a block diagram at the top of Fig.12. Once T_m is obtained, it will be sent to D/A to convert into a torque reference command voltage between 0 to 10V. This command will be passed to the torque controlled inverter to drive the motor [10], [11].

5. EXPERIMENTAL RESULTS

Three experiments were conducted on the wind turbine simulator: 1) determination of the wind turbine characteristic, 2) load perturbation and 3) wind speed simulation. Figure 13 shows power-speed curves at different wind speeds (4, 4.5, 5 and 5.5 m/s). The solid lines in the figure are obtained from the calculation using Equation (6) whereas the diamond and plus symbols represent the measurement from the experiment. Figure 14 shows a plot of power coefficient, c_P , and λ . The solid line inside the graph is calculated based on Equations (6) and (7). The plus signs stand for power coefficient of the wind turbine. As can be seen from the two figures, there is a good agreement between the calculation and measurement from the simulator. The results verify that the wind turbine simulator can reproduce the steady-state characteristics of a given wind turbine at various wind conditions.

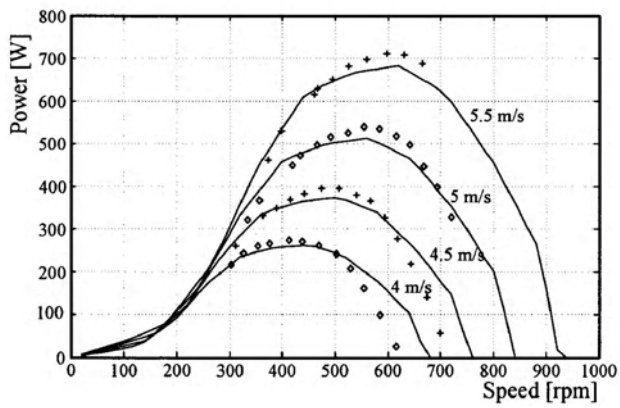

Fig. 13. Characteristics of a wind turbine simulator (◊ and +) and calculated results.

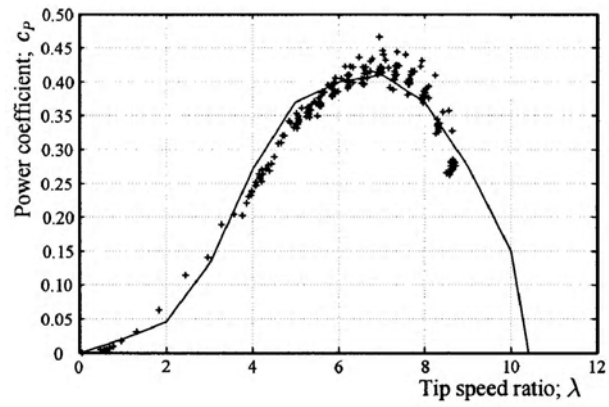

Fig. 14. Power coefficient of the wind turbine simulator compared with that of the real 3kW wind turbine.

The power response of the wind turbine simulator on the 1 kW wind turbine system is shown in Fig. 15. At the beginning $t = 0$, the reference power was raised to accelerate the wind turbine. The output power in Fig. 15(b) increased and reached steady state condition at $t = 70$. At $= 220$, the load disturbance is stepped up to 750 W, as seen from a jump in the output power. In each step of the load increase at $t = 0$ and 220, the controller of the wind turbine took a few seconds to track the output power until it matched the reference power (Fig. 15(a)). Figure 15(c) displays the error between the reference power and output power.

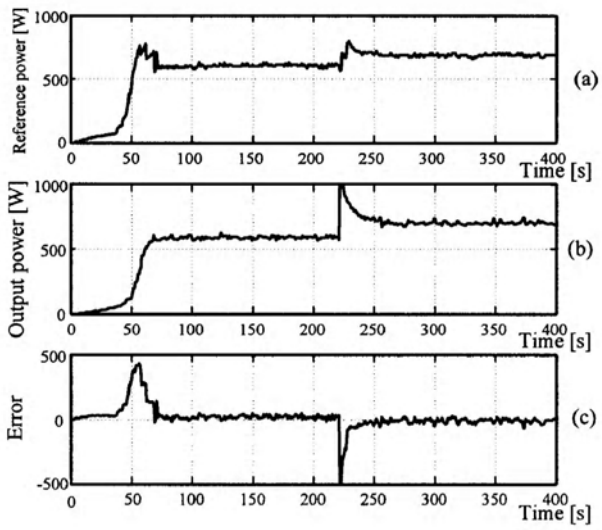

Fig. 15. Power response of the wind turbine simulator to a step increase and load disturbance: (a) reference power (b) output power of induction motor, (c) error signal.

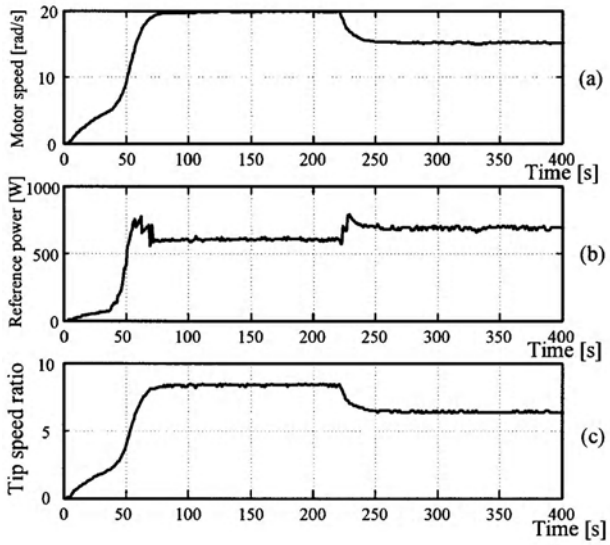

Fig. 16. Responses to load perturbation: (a) motor speed, (b) reference power, (c) tip speed ratio.

The response of tip speed ratio and motor speed for the same condition as in Fig. 15 is shown in Fig. 16. It can be seen that at t=220, both motor speed and tip speed ratio decrease, as indicated by the characteristic of Fig. 4. Figure 17 illustrates that the power coefficient increases when the system load is stepped up to 750 W. Figure 18 presents the output torque response for the same operating conditions, confirming that the controller is capable of tracking the reference torque calculated from (7) effectively. It can be concluded from Fig. 15-18 that the digital controller of the wind turbine simulator gives very satisfactory steady performance.

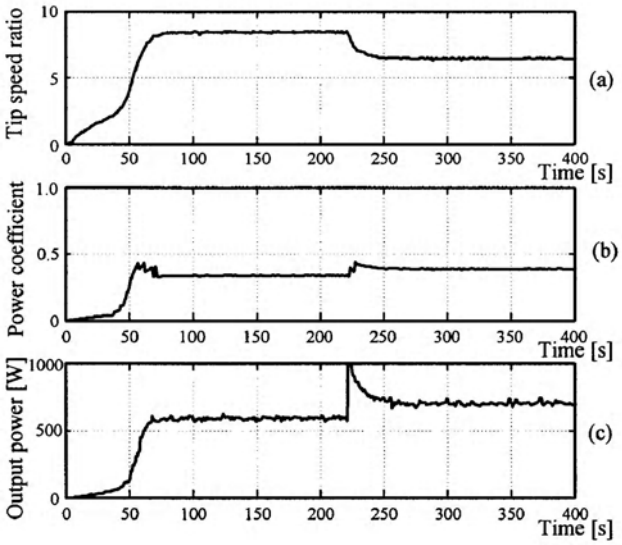

Fig. 17. Responses to load perturbation: (a) tip speed ratio, (b) power coefficient, (c) output power of induction motor.

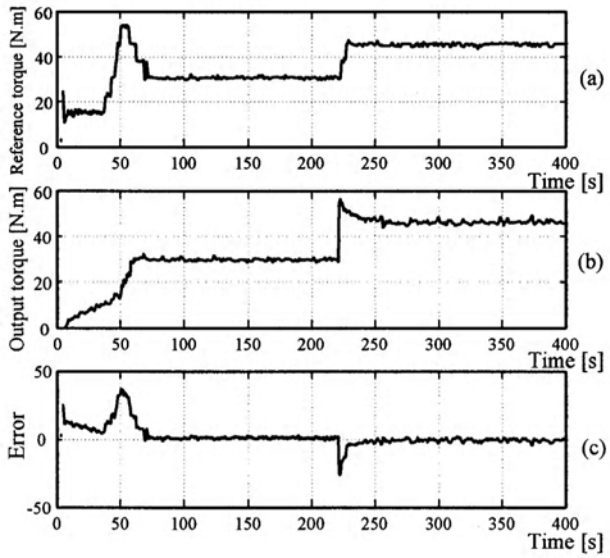

Fig. 18. Torque response to load increase: (a) reference torque, (b) output torque, (c) error between the reference and output torques.

An experiment on the tower effect was conducted with a constant load of 130 W and a constant wind speed of 5 m/s. The result is shown in Figure 19. In this experiment, the wind turbine was assumed to have three-blades, and therefore the torque ripple occurred every $2\pi / 3$ rad.

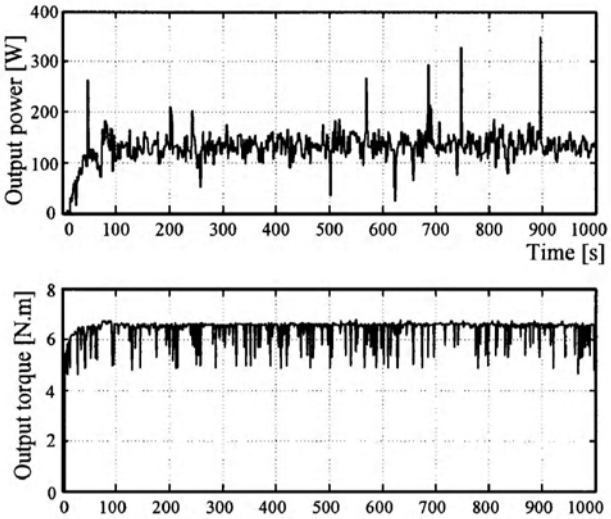

Fig. 19. Tower effect on: (a) output power and (b) output torque.

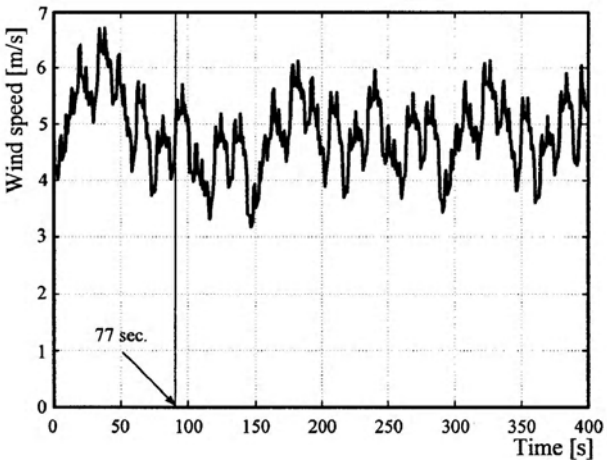

Fig. 20. Simulation of the wind speed based on Van der Hoven spectrum for a period of 400 sec.

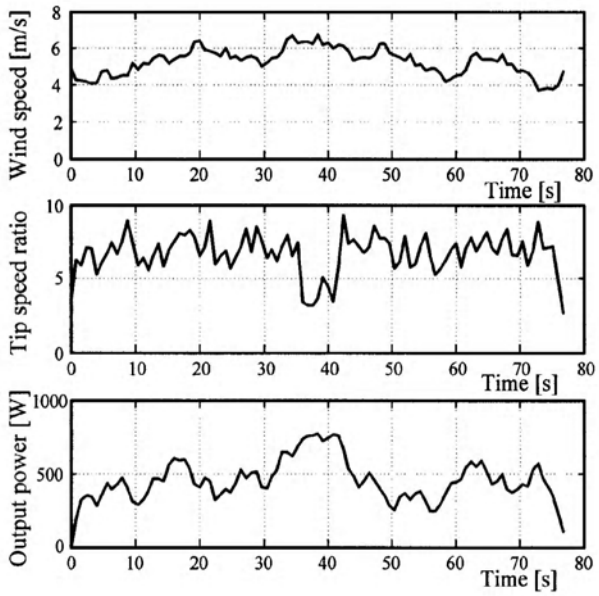

Fig. 21. (a) wind speed, (b) output power and (c) aerodynamic torque between 0-77 seconds of the wind speed profile in Fig. 20.

Figure 20 shows time-series wind speed for a period of 400 sec. The wind speed is simulated by the Van der Hoven power spectrum implemented with MATLAB. The input parameters used in the model are as follows: A_0 = 4.5 m/s, N =55, and $\omega_i = i \times 10^k$ [rad/h] for i = 1, 2,…, 9 and k = -2, -1, 0, 1, 2 (refer to Equations (1) and (2)). These wind speed data will be passed and served as input data for the DSC board. Figure 21 is a closer look of the wind speed profile in the first 77 seconds. The corresponding tip speed ratio and output power are also provided in the figure.

6. CONCLUSIONS

The development of wind turbine simulator for wind power plant testing is presented. The developed simulator was implemented by a low-cost, high-performance DSC controller developed by C language. Wind speed can be easily programmed based on the Van der Hoven power spectrum, or from recorded wind speed data or from manual set-up. The advantages of the simulators are that various wind profiles and wind turbines can be incorporated as desired in the control software and it includes the data acquisition to verify the control algorithms and display the parameters. The experimental results confirmed the wind turbine simulator can perform satisfactorily under steady state wind profile, turbulence and tower effect. The system could provide all necessary parameters of the wind turbine system such as wind speed, output torque, torque coefficient, output power, power coefficient, and tip speed ratio.

NOMENCLATURE

A_{turb}	=	swept area of the turbine [m^2]
f	=	frequency [Hz]
$c_P^{\max}$	=	maximum power coefficient [pu]
$c_T^{\max}$	=	maximum torque coefficient [pu]
D	=	tower diameter [m]
G	=	gear ratio [pu]
J_g	=	inertia of generator [kg.m^2]
J_m	=	inertia of motor [kg.m^2]
J_t	=	inertia of turbine [kg.m^2]
N	=	sampling operation
P	=	output power of turbine [W]
R	=	radius of blade of blade [m]
T_{f1}	=	friction torque of wind turbine system [N.m]
T_{f2}	=	friction torque of M-G set [N.m]
T_{comp}	=	compensation torque [N.m]
T_g	=	generator torque [N.m]
T_m	=	motor torque [N.m]
T_{tower}	=	tower effect turbine ripple [N.m]
T'_{turb}	=	turbine torque without tower effect [N.m]
T_{turb}	=	turbine torque [N.m]
$\overline{v}$	=	mean wind speed [m/s]
ρ	=	air density [kg/m^3]
α_t	=	angular acceleration of turbine [rad/s^2]

β = pitch angle [rad]

φ_i = phase angle with uniformly distributed random number in a domain of [rad].

ω_0 = starting radian frequency [rad/s]

ω_g = angular velocity of generator [rad/s]

ω_t = angular velocity of turbine [rad/s]

REFERENCES

[1] Nichita, C.; Luca, D.; Dakyo, B.; Ceanga, E. 2002. Large Band Simulator of Wind Speed for Real Time Wind Turbine Simulators. *Energy Conversion, IEEE Tran.* 17(4): 523-529.

[2] I. Munteanu; N. A. Cutululis; A. I. Bratcu; E. Ceanga. 2004. Optimization of variable speed wind power systems based on a LQG approach. *ELSEVIER Tran.* on Control Engineering Practice.

[3] J.F. Manwell; J.G. McGowan and A. L. Rogers. 2004. *Wind Energy Explained*, John Wiley & Sons, England.

[4] Kojabadi, H.M.; Liuchen Chang; Boutot, T. 2004. Development of a Novel Wind Turbine Simulator for Wind Energy Conversion Systems Using an Inverter-Controlled Induction Motor. *Energy Conversion, IEEE Tran.* 19 (3): 547 – 552.

[5] Hossein Madadi Kojabadi, Liuchen Chang and Tobie Boutot. 2004. *Development of a Novel* Wind Turbine Simulator for Wind Energy Conversion Systems Using an Inverter-Controlled Induction Motor, *IEEE Energy Conversion* 19(3): 547-552.

[6] H. Vihrial. 2002. *Control of Variable Speed Wind Turbines*. Ph.D Thesis, Tampere University of Technology.

[7] Erich Hau. 2002. *Wind turbines*, Spring-Verlag Berlin Heidelberg, 139-144.

[8] T. Thiringer; J. A. Dahlberg. 2001. Periodic Pulsations from a Three-Bladed Wind Turbine. *Energy Conversion, IEEE Tran.* 16 (2): 128-133.

[9] Seung-Ho SOng; Byoung-Chang Jeong; Hye-In Lee; Jeong-Jae Kim; Jeong-Hun Oh; Venkataramanan, G. 2005. Emulation of output characteristics of rotor blades using a hardware-in-loop wind turbine simulator. *Applied Power Electronics Conference and Exposition, APEC 2005. Twentieth Annual IEEE* 3, 6-10 March: 1791-1796.

[10] P.E. Battaiotto; R.J. Mantz and P.F. Puleston. 1996. A Wind Turbine Emulator Based on a Dual DSP Processor System, *Control Eng. Practice* 4 (9): 1261-1266.

[11] David Parker. 2002. Computer Based Real-Time Simulator for Renewable Energy Converters, *Proceedings of the First IEEE International Workshop on Electronic Design Test and Applications.*